Journal of Catalysis **194,** 33–44 (2000)
doi:10.1006/jcat.2000.2907, available online at http://www.idealibrary.com on IDEAL®

Characterization of Pd/C and Cu Catalysts for the Oxidation of Methane to a Methanol Derivative

Eun Duck Park, Sun Hee Choi, and Jae Sung Lee[1]

Department of Chemical Engineering and School of Environmental Engineering, Pohang University of Science and Technology (POSTECH), San 31 Hyoja-Dong, Pohang 790-784, Republic of Korea

Received September 24, 1999; revised April 21, 2000; accepted April 25, 2000

Carbon-supported Pd catalysts with a copper compound for the oxidation of methane to a methanol derivative, CF_3COOCH_3, in the presence of CO and O_2 were characterized. The bulk structure and chemical environment of palladium and copper were determined by XRD and XAFS, respectively. In this reaction system, the nature of cocatalyst, the presence of Cl^-, and the solvent composition changed the structure of the palladium species and affected the yield of CF_3COOCH_3. In the presence of a copper compound and Cl^-, the metallic palladium can be partly oxidized into Pd(II) species, which resulted in higher yields of CF_3COOCH_3. For the active catalyst system, the copper compound was present as CuCl. Pd(II) species coordinated with Cl^- appeared to be essential for the selective activation of methane and the metallic palladium for the *in situ* generation of H_2O_2 from CO, H_2O, and O_2.

Key Words: **methane oxidation; methanol; Pd/C; copper; chlorine ion; XAFS; XRD.**

INTRODUCTION

One of nature's great challenges to the scientist is the selective oxidation of methane (the primary component in natural gas) to methanol or other efficiently transportable materials. There have been a number of reported catalyst systems that have the potential to serve the purpose in the gas phase and/or in the liquid phase but few have been found to be attractive in an economic viewpoint (1). Recently, metal-catalyzed systems in protic media attract much attention because highly selective and productive functionalizations of methane have been accomplished (2–7). One of these metal compounds, palladium, also has been reported to be active for the oxidative carbonylation (8–15), partial oxidation (16–31), and carboxylation reaction (32–35) in the presence of cocatalyst as a redox partner. Despite a number of reports on the reaction itself, characterization of these various redox systems containing palladium as a main active component has been limited. For the oxidative carbonylation of phenol, Takagi *et al.* (15) studied a novel catalyst of Pd/C–Pb–NMe_4Br with ICP analysis and reported that the Pd species seemed to work as a homogenous catalyst. For the oxidation of carbon monoxide over supported $PdCl_2$–$CuCl_2$ catalysts, IR (22), XRD (23–27), and XAFS (27–31) studies have indicated that the reaction scheme appears similar to that of homogeneous Wacker processes even over the supported catalyst system. Fujiwara's group (35) studied a homogeneous $Pd(OAc)_2$–$Cu(OAc)_2$–$K_2S_2O_8$–CF_3COOH (TFA) system which leads to the carboxylation of small alkanes. They observed the change in the electronic state of palladium in the presence of Cu salts with visible–UV spectroscopy and electron spectroscopy for chemical analysis (ESCA).

Sen and co-workers have reported the activation of small hydrocarbons (4–7) and decomposition of highly toxic molecules (36–38) over Pd-based catalyst systems in the presence of CO and O_2. Recently, they employed 5% Pd/C and soluble copper(II) salts in a mixture of trifluoroacetic acid (TFA) and water and observed the selective oxidation of methane and other lower alkanes by dioxygen (6). In this system, carbon monoxide must also be present in the reaction mixture in order to maintain a high selectivity to partially oxidized products in the reaction. The necessity of a co-reductant bears a striking resemblance to reactions of monooxygenase enzymes (e.g., cytochrome P450), which requires a reducing agent such as NADH to activate O_2 and effect oxidation of substrates (39). The characteristics of the reaction show that this catalyst system is quite different from the previously reported catalyst systems of Pd and a second metal. In spite of these interesting findings, works to correlate the catalytic activity with the structure of catalyst have not been accomplished yet. In this work, we characterized the similar catalyst system and attempted to find the correlation between the catalyst structure and the catalytic activity and selectivity in functionalization of methane.

[1] To whom correspondence should be addressed. Fax: 82-562-279-5799. E-mail: jlee@postech.ac.kr.

0021-9517/00 $35.00

EXPERIMENTAL

Catalysts

5% Pd/C (Alfa) was purchased and utilized after reduction at 473 K in the dihydrogen streams. 5% Pd/AC catalysts were prepared by the wet impregnation method from $Pd(NO_3)_2$ and activated carbon (AC, BET surface area, 1075 m^2/g) followed by reduction at different temperatures. As inorganic cocatalysts, $CuCl_2 \cdot 2H_2O$ and $Cu(CH_3COO)_2$ with or without NaCl were utilized.

Reactions

Given amounts of Pd catalyst, an inorganic cocatalyst, and TFA and/or water as solvent were charged into a 300-ml autoclave reactor (Parr) with a glass liner. CO, O_2, N_2, and CH_4 were successively charged and the reaction temperature was adjusted to 353 K or 373 K. Reaction products were identified by GC–mass (HP 5971 MSD) and quantified by gas chromatography (HP 5890 GC) by comparison with authentic samples. The reaction rates were expressed in site time yield (STY) defined as the moles of selective oxidation products (CF_3COOCH_3 and HCOOH) formed per mole of Pd per second.

Characterization of Catalysts

The XAFS (X-ray absorption fine structure) spectra were taken in transmission mode for the K-edges of Pd and Cu at beamline 10B of the Photon Factory in the National Laboratory for High Energy Physics (KEK) operating at 2.5 GeV with ca. 250–350 mA of stored current (40–42). Catalysts were evacuated at 333 K to remove solvents after the reaction and transferred into an EXAFS cell with Kapton windows and the cell was sealed. In the case of Cu samples, it was difficult to make such thin XAFS sample wafers that would give an optimal X-ray absorption because of high Cu loadings. Thus, samples after measuring Pd K-edge XAFS were exposed to air just before the measurement of Cu spectra to minimize the exposure time. The spectra were taken in a transmission mode at room temperature. Ionization chambers were used for measuring beam intensities. For Cu samples, the detector gases were N_2 (100%) for the incident beam and N_2 (85%) + Ar (15%) for the transmitted beam, and in the measurement of Pd samples Ar (100%) gases were used for both detectors. In addition to catalyst samples, XAFS data were also obtained for Pd foil, $PdCl_2$, $Pd(CH_3COO)_2$, and PdO samples as Pd references and Cu foil, CuCl, $Cu(CH_3COO)_2$, and $CuCl_2 \cdot 2H_2O$ as Cu references. The obtained XANES (X-ray absorption near-edge structure) spectra were analyzed in a VAX/VMS operating system by UW5 package, and EXAFS (extended X-ray absorption fine structure) data were analyzed by using the UWXAFS 3.0 package and FEFF 7.0 code licensed from the University of Washington (43). The XAFS data were first subject to pre-edge subtraction so as to remove the effects due to absorption by another edge of the absorber or by other components. The pre-edge region was fitted with a simple line and extrapolated beyond the edge. The interference function of EXAFS is defined as $\chi(E) = [\mu(E) - \mu_o(E)]/\Delta\mu_o(E_o)$ above the absorption edge (E_o) where $\mu(E)$ is the absorption coefficient due to particular edge of the element of interest in the sample, $\mu_o(E)$ is the atomic-like absorption, and $\Delta\mu(E_o)$ is the jump at the edge. Unmeasured $\mu_o(E)$ is approximated by a piecewise spline that can be adjusted so that low R-components of Fourier transformed data ($\chi(R)$) are optimized. The scaled EXAFS function $k^3\chi(k)$ of momentum (k) space was converted to real space, i.e., R-space, by Fourier transformation, resulting in the radial structural function (RSF) of the sample. For Fourier transformation, k_{min} was chosen between 1.20 and 2.00 $Å^{-1}$ and k_{max} between 12.25 and 14.25 $Å^{-1}$ with Hanning window sills.

The nonlinear EXAFS fitting was performed in R-space without Fourier filtering. The standards were Pd–Pd and Pd–Cl single scattering that were synthesized with the FEFF code by using structural information on Pd metal (44) and $PdCl_2$ (45). A single adjustable parameter in XAFS analysis, amplitude reduction factor (S_o^2), was taken to be 0.88 for Pd, which was found by fitting experimental RSFs of Pd foil with a theoretical one.

X-ray powder diffraction patterns were obtained at room temperature using a M18XHF (MAC Science Co.) with Ni-filtered Cu $K\alpha$ radiation (1.54056 Å). The X-ray tube was operated at 40 kV and 200 mA. Samples were prepared as done for XAFS techniques and packed into a glass holder having an 18- × 18- × 2-mm opening. No adhesive or binder was necessary. The 2θ angle was scanned at a rate of 4° min^{-1}. To obtain an average particle size, a line broadening analysis of XRD peaks was performed using the Scherrer equation (46).

RESULTS

Homogeneous Pd Catalyst vs Heterogeneous Pd/C

The functionalization of methane over this catalyst system proceeds according to the overall stoichiometry represented by reaction [1]:

$$CH_4 + CF_3COOH + CO + O_2 \rightarrow CF_3COOCH_3 + H_2O + CO_2. \quad [1]$$

This reaction has been reported to occur with formation of by-products that include the hydrolysis product of CF_3COOCH_3 such as methanol and further oxidized products such as HCOOH and CO_2 (6). Throughout our experiments, HCOOH was observed as the major by-product. The yield of HCOOH was generally proportional to that of CF_3COOCH_3. Related to carbon monoxide, there is a side

TABLE 1

Effects of Various Palladium and Copper Compounds in the Homogeneous System[a]

Run	Pd compound	Cu compound	Oxidation products/mmol		STY[b] × 10^4
			CF_3COOCH_3	HCOOH	
1	$PdCl_2$	—	—	—	—
2	—	$CuCl_2$	—	—	—
3	$PdCl_2$	$CuCl_2$	0.41	0.19	5.9
4	$Pd(CH_3COO)_2$	$Cu(CH_3COO)_2$	0.04	0.11	1.5
5	$Pd(CH_3COO)_2$	$CuCl_2$	0.46	0.50	9.5
6	$PdCl_2$	CuCl	0.47	0.49	9.5
7	$PdCl_2$	$Cu(CH_3COO)_2$	0.52	0.40	9.1

[a] Pd, 0.0564 mmol; Cu, 0.1 mmol; H_2O, 1 ml; CF_3COOH, 3 ml; CH_4, 400 psi; CO, 200 psi; O_2, 100 psi; 353 K; after 5 h.
[b] Site time yield (STY) is defined as the moles of oxidation products per moles of Pd per second.

reaction [2]:

$$CO + \tfrac{1}{2}O_2 \rightarrow CO_2. \qquad [2]$$

This is the complete CO oxidation catalyzed by Pd(II) species following well-known Wacker chemistry.

The effects of various palladium and copper compounds were examined in the homogeneous system as shown in Table 1. Palladium or copper compound alone gave much lower yields of CF_3COOCH_3 than those obtained in the presence of both compounds. Even in the latter case, the yield increased when Cl^- was present as a ligand for the Pd or Cu compound.

For the potential advantage in practical applications, carbon-supported Pd catalyst was introduced as a heterogeneous catalyst and compared to the homogeneous $PdCl_2$ catalyst. As shown in Table 2, both catalysts showed similar yields of CF_3COOCH_3 with the same amount of Pd as long as the metallic palladium was well dispersed (run 2 in Table 2). For carbon-supported Pd catalysts, increasing reduction temperatures gave larger particle sizes of palladium, lower CO conversions, and lower yields of CF_3COOCH_3. Thus, the particle size of palladium appears to be closely related to the yield of CF_3COOCH_3.

Effect of Cl^-

In this catalyst system, the presence of a copper compound as a cocatalyst was proved to be essential (6). In addition, the yield of CF_3COOCH_3 increased with the amount of Cl^- added as NaCl as shown in Table 3. However, an excessive amount of NaCl (in case of [NaCl]/[Pd] = 100) gave a higher CO conversion but had an adverse effect on the yield of CF_3COOCH_3.

XRD was conducted to observe the change in the bulk structure of palladium and copper during the reaction. In Fig. 1, the peak at 2θ of 40° represents the Pd(111) plane. Its intensity increased after the reaction in the absence of $Cu(CH_3COO)_2$ and NaCl, indicating the growth of the size of palladium metal. The crystal sizes of palladium calculated by the Scherrer equation from line-broadening of the Pd(111) plane were 6.5 nm and 36.6 nm before and after the reaction, respectively. However, this peak height decreased in the presence of $Cu(CH_3COO)_2$ and NaCl. As the amount

TABLE 2

Activity Comparison between Homogeneous $PdCl_2$ and Heterogeneous Pd/C Catalysts[a]

Run	Pd catalyst	Particle size[b] *d*/nm	Oxidation products/mmol		STY[c] × 10^3	CO conversion (%)
			CF_3COOCH_3	HCOOH		
1	$PdCl_2$ (homogeneous)	—	0.70	0.74	8.0	67
2	5% Pd /C, 473 K	6.5	0.69	0.62	7.3	63
3	5% Pd/AC, 673 K	12.6	0.60	0.61	6.7	56
4	5% Pd/AC, 873 K	36.6	0.53	0.51	5.8	50

[a] 5% Pd/C, 21.5 mg (Pd, 1.0×10^{-5} mol) or $PdCl_2$ (1.0×10^{-5} mol), $Cu(CH_3COO)_2$ (5.0×10^{-5} mol), NaCl (1.5×10^{-4} mol); H_2O, 1 ml; CF_3COOH, 3 ml; CH_4, 300 psi; N_2, 100 psi; CO, 200 psi; O_2, 100 psi; 373 K; after 5 h.
[b] By X-ray line broadening.
[c] Same definition as described in Table 1.

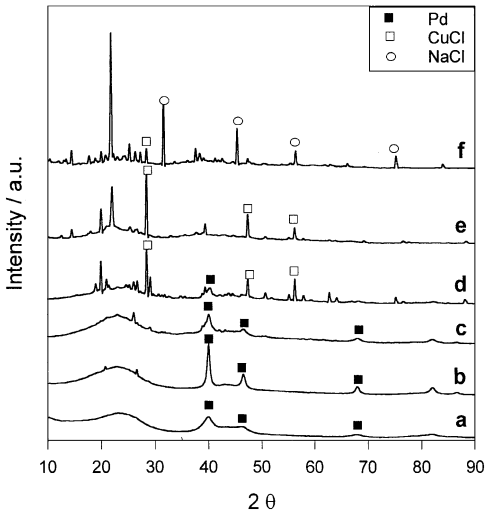

FIG. 1. X-ray diffractogram of 5% Pd/C catalyst system reduced at 473 K before (a) and after the reaction (b) in the absence of $Cu(CH_3COO)_2$ and after the reaction under different mole ratios of NaCl relative to Pd of 0 (c), 5 (d), 15 (e), and 100 (f) in the presence of $Cu(CH_3COO)_2$ ([Cu]/[Pd] = 5); the solvent composition and reaction conditions were the same as those in Table 2.

of NaCl increased at a fixed amount of $Cu(CH_3COO)_2$ (mole ratio of Cu/Pd = 5), peaks representing CuCl became strengthened. When an excessive amount of NaCl was used ([NaCl]/[Pd] = 100), sharp peaks representing NaCl were also observed.

In order to obtain information on the chemical state of Pd and Cu species in these catalysts during the reaction with different amounts of Cl^-, the technique of XANES was employed. Figure 2 compares Pd K-edge XANES of

TABLE 3

Effect of the Amount of NaCl for the Carbon-Supported Pd Catalyst System [a]

[NaCl]/[Pd]	Oxidation products/mmol		STY[b] × 10^3	CO conversion (%)
	CF_3COOCH_3	HCOOH		
0.00	—	—	—	16
0.50	0.21	0.41	3.4	27
1.00	0.25	0.42	3.7	40
3.50	0.27	0.57	4.7	44
5.00	0.50	0.60	6.1	50
7.50	0.48	0.70	6.6	54
10.0	0.58	0.79	7.6	57
15.0	0.69	0.62	7.3	63
100	0.29	0.24	2.9	68

[a] 5% Pd/C, 21.5 mg (Pd, 1.0×10^{-5} mol), $Cu(CH_3COO)_2$ (5.0×10^{-5} mol); H_2O, 1 ml; CF_3COOH, 3 ml; CH_4, 300 psi; N_2, 100 psi; CO, 200 psi; O_2, 100 psi; 373 K; after 5 h.

[b] Same definition as described in Table 1.

carbon-supported Pd catalysts before and after the reaction with those of some reference compounds, Pd foil, $PdCl_2$, $Pd(NO_3)_2$, PdO, and $Pd(CH_3COO)_2$. The maximum absorption edge in each spectrum corresponds to the allowed $1s \rightarrow 5p$ transition. Pd references show easily differentiated shapes of their respective XANES. All catalysts except the one with [NaCl]/[Pd] = 15 showed XANES shapes similar to that of Pd metal. Only the catalyst containing the high amount of NaCl showed XANES shape similar to that of $PdCl_2$.

In the case of Cu species, Fig. 3 compares Cu K-edge XANES of catalysts after the reaction with different amounts of NaCl with those of some reference compounds,

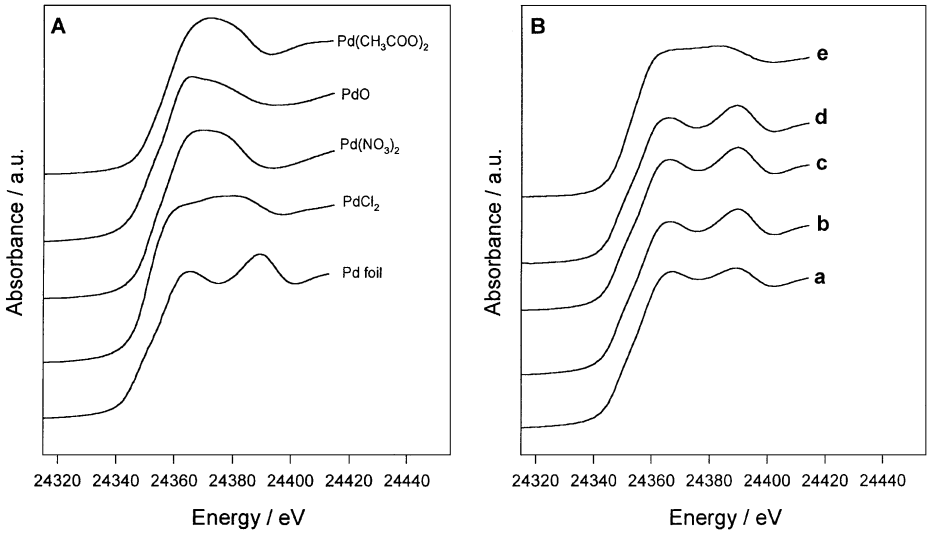

FIG. 2. Pd K-edge XANES of Pd references (A) and 5% Pd/C catalyst system (B) before (a) and after the reaction (b) in the absence of $Cu(CH_3COO)_2$ and after the reaction under different mole ratios of NaCl relative to Pd of 0 (c), 5 (d), and 15 (e) in the presence of $Cu(CH_3COO)_2$ ([Cu]/[Pd] = 5); the solvent composition and reaction conditions were the same as those in Table 2.

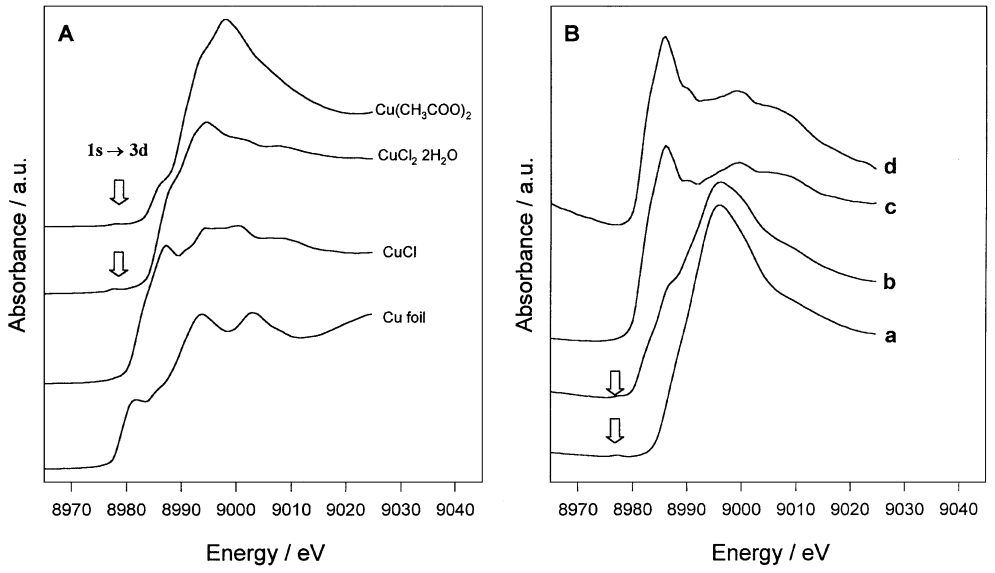

FIG. 3. Cu K-edge XANES of Cu references (A) and 5% Pd/C catalyst system (B) after the reaction under different mole ratios of NaCl relative to Pd of 0 (a), 5 (b), 15 (c), and 100 (d) in the presence of $Cu(CH_3COO)_2$ ([Cu]/[Pd] = 5); the solvent composition and reaction conditions were the same as those in Table 2.

Cu foil, CuCl, $CuCl_2 \cdot 2H_2O$, and $Cu(CH_3COO)_2$. As discussed elsewhere (26–31), the absorbance maximum is assigned to the allowed $1s \rightarrow 4p$ transition. Below the maximum are subsidiary peaks and shoulders reflecting transitions to empty orbitals according to the dipole selection rule. A very weak peak below the edge at 8978 eV in $CuCl_2 \cdot 2H_2O$ and $Cu(CH_3COO)_2$ represents the quadruple-allowed $1s \rightarrow 3d$ transition, which serves as a signature of a Cu(II) compound since there is no $3d$ hole in Cu(0) or Cu(I) compounds. This very weak peak is also found for catalysts after the reaction in the absence of NaCl. However, this peak became weakened and disappeared as the amount of NaCl increased. Therefore, a majority of copper species present in catalysts without NaCl seems to be Cu(II) compounds. However, as the amount of NaCl increased, Cu(II) compounds were reduced to Cu(I) compound as also observed in XRD results. The $1s \rightarrow 4s$ peak in Cu(II) compounds appears at 8985 eV as a shoulder with greatly reduced intensity. The edge positions of Cu references were determined to be 8979.0 eV, 8982.0 eV, 8985.7 eV, and 8984.7 eV for Cu foil, CuCl, $CuCl_2 \cdot 2H_2O$, and $Cu(CH_3COO)_2$, respectively, and reflected the shift to a higher energy as the oxidation number was raised. The edge positions of Cu samples were determined to be 8987.0 eV, 8981.8 eV, 8982.0 eV, and 8981.3 eV for four samples shown in Fig. 3B-a–d, respectively. This shift in edge position also showed the reduction of Cu(II) compounds into Cu(I) compounds as the amount of NaCl increased.

To obtain information about the structure around the Pd atom, small oscillations above the absorption edge were isolated to produce the EXAFS function $\chi(k)$ and RSF for Pd references and samples under different catalyst compositions. Major peaks in the RSF correspond to important interatomic distances shifted from their true position by a phase shift and their intensities are correlated with the average coordination number of the atom at the distance. Palladium references in Fig. 4 have different oscillations

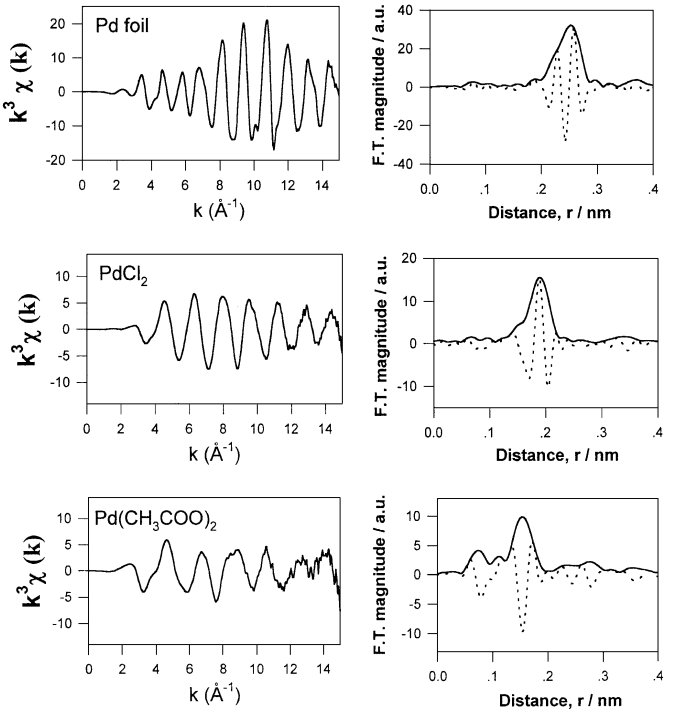

FIG. 4. k^3-weighted EXAFS functions and their Fourier transformation about the Pd K-edge of Pd references. The imaginary parts are plotted as dotted lines.

in $\chi(k)$ and different phase-uncorrected distance peaks in RSF. In particular, the imaginary part of the Fourier transform clearly characterizes the nature of palladium by comparison of its shape and the number of peaks. From these results, it can be derived that peaks at 0.252 nm, 0.187 nm, and 0.153 nm represent Pd–Pd, Pd–Cl, and Pd–O interactions, respectively. Figure 5 shows the Pd K-edge EXAFS spectra of samples before (Fig. 5a) and after (Fig. 5b) the reaction in the absence of $Cu(CH_3COO)_2$ and NaCl. In all cases, only peak at 0.252 nm could be observed, indicating that the metallic palladium was the dominant Pd species during the reaction. The intensity of this peak, and thus the coordination number of Pd–Pd, increased compared with that of the fresh catalyst after the reaction. EXAFS fitting results summarized in Table 4 showed that the coordination number increased from 7.1 to 8.7. This is consistent with the result observed in XRD patterns.

The effects of Cl^- on the structure of palladium were studied with EXAFS. Figure 6 shows the Pd K-edge EXAFS spectra of samples with different amounts of NaCl at a fixed amount of $Cu(CH_3COO)_2$ (Cu/Pd = 5). Compared with Pd references, two peaks at 0.187 nm and 0.252 nm in Fig. 6 can be assigned to Pd–Cl and Pd–Pd interactions, respectively. In the absence of NaCl, the peak representing the Pd–Pd interaction increased after the reaction (Fig. 6a) compared with that of the fresh catalyst (Fig. 5a). Thus the coagulation of Pd occurred under the reaction conditions. However, as

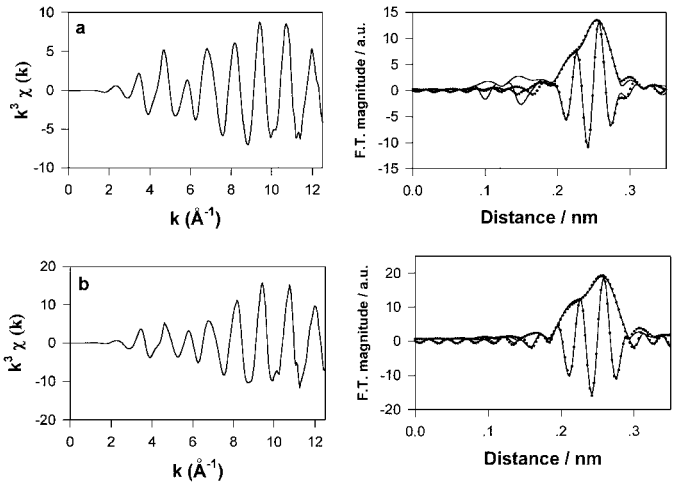

FIG. 5. k^3-weighted EXAFS functions and their Fourier transformation with the imaginary part about the Pd K-edge of 5% Pd/C catalyst system before (a) and after the reaction (b). The EXAFS fitting results are plotted as dots. The solvent composition and reaction conditions were the same as those in Table 2.

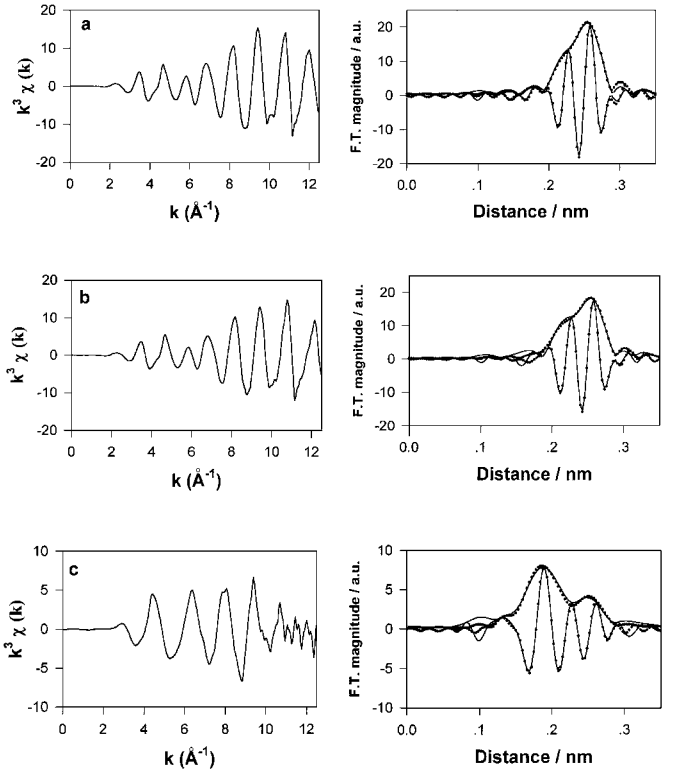

FIG. 6. k^3-weighted EXAFS functions and their Fourier transformation with the imaginary part about the Pd K-edge of 5% Pd/C catalyst system after reaction with different amounts of NaCl at a fixed amount of $Cu(CH_3COO)_2$ ([Cu]/[Pd] = 5) as a chlorine source. The EXAFS fitting results are plotted as dots; [NaCl]/[Pd] = 0 (a), 5 (b), and 15 (c). The solvent composition and reaction conditions were the same as those in Table 2.

TABLE 4

Pd K-Edge EXAFS Curve-Fitting Results of Carbon-Supported Pd Catalysts under Different Catalyst Compositions and Solvent Compositions

Catalyst shown in figures	Shell	N	R (Å)	σ^2 (Å^2)	R-factor
Fig. 5a	Pd	7.1	2.737	0.0074	0.0018
Fig. 5b	Pd	8.7	2.739	0.0058	0.0026
Fig. 6a	Pd	9.2	2.740	0.0062	0.0023
Fig. 6b	Pd	7.7	2.740	0.0059	0.0020
	Cl	0.3	2.360	−0.0032	
Fig. 6c	Pd	1.5	2.747	0.0044	0.0052
	Cl	3.0	2.323	0.0051	
Fig. 10a	Pd	4.0	2.741	0.0049	0.0053
	Cl	0.9	2.350	0.0028	
Fig. 10b	Pd	1.1	2.745	0.0023	0.0053
	Cl	1.1	2.376	0.0030	
Fig. 11a	Pd	8.8	2.735	0.0067	0.0019
Fig. 11b	Pd	6.0	2.737	0.0059	0.0054
	Cl	1.5	2.315	0.0050	
Fig. 13a	Cl	4.0	2.302	0.0030	0.0055
Fig. 13b	Pd	0.3	2.730	0.0013	0.0013
	Cl	2.7	2.346	0.0046	

Note: R-factor gives a sum-of-squares measure of the fractional misfit, which is defined as $R = \frac{\sum_{i=1}^{N}\{[Re(f_i)]^2 + [Im(f_i)]^2\}}{\sum_{i=1}^{N}\{[Re(\chi_{\mathrm{data}_i})]^2 + [Im(\chi_{\mathrm{data}_i})]^2\}}$.

the amount of NaCl increased, the peak at 0.252 nm became weakened and a new peak at 0.187 nm representing a Pd–Cl interaction appeared and became strengthened. The addition of NaCl changes the structure of palladium. At low concentrations of NaCl ([NaCl]/[Pd] = 5), the effect of chlorine is not clearly seen in $\chi(k)$ and RSF (Fig. 6b). However, for the sample containing a higher [NaCl]/[Pd] ratio of 15 (Fig. 6c), the oscillation in $\chi(k)$ and peak shape in RSF have a distinct difference compared with the sample without Cl^-. The $\chi(k)$ spectrum of this sample is very close to that of $PdCl_2$ in Fig. 4. The EXAFS fitting results in Table 4 make clearer the influence of Cl^-. The coordination number of Pd–Pd increased from 7.1 to 9.2 after the reaction in the absence of NaCl. However, the coordination number of Pd–Cl appeared in the presence of NaCl and its value increased as the amount of NaCl increased whereas the coordination numbers of Pd–Pd decreased. Therefore, increasing amounts of NaCl seem to cause the transition of palladium from the metallic state into the ionic state coordinated with Cl^-.

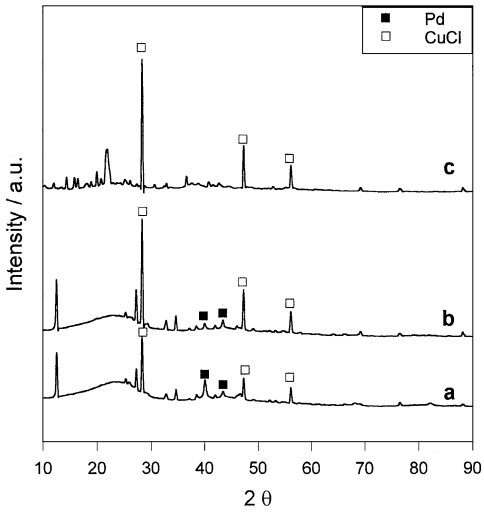

FIG. 7. X-ray diffractogram of 5% Pd/C catalyst system with different mole ratios of $CuCl_2$ relative to Pd of 2.5 (a), 5.0 (b), and 50 (c). The solvent composition and reaction conditions were the same as those in Table 2.

Effect of $CuCl_2$

Compared with $Cu(CH_3COO)_2$ and NaCl, $CuCl_2$ is believed to have the combined effects of them. The yield of CF_3COOCH_3 increased with the amount of $CuCl_2$ as shown in Table 5. However, an excessive amount of $CuCl_2$ (in the case of [Cu]/[Pd] = 50) had an adverse effect on the yield of CF_3COOCH_3.

XRD was conducted to observe the change in the bulk structure of palladium and copper during the reaction with different amounts of $CuCl_2$. As shown in Fig. 7, the peak at 2θ of 40° representing the Pd(111) plane became weakened as the amount of $CuCl_2$ increased. In all cases, peaks representing CuCl were observed by XRD as the only copper phase.

XANES spectra were observed in order to obtain information on the chemical state of Pd and Cu species in these catalysts during the reaction with different amounts of $CuCl_2$. Figure 8 compares Pd K-edge XANES of carbon-supported Pd catalysts before and after the reaction. Compared with Pd references in Fig. 2A, the general shapes of XANES of samples became similar to that of $PdCl_2$ as the amount of $CuCl_2$ increased. To find out the difference in the effect of $CuCl_2$ on the metallic palladium of different particle sizes, Pd/AC reduced at 673 K was prepared and characterized before (Fig. 8c) and after the reaction (Fig. 8d). This catalyst contains Pd of larger particle sizes compared with the commercial Pd/C catalyst. Pd K-edge XANES spectra

TABLE 5

Effect of Amount of $CuCl_2$ for the Carbon-Supported Pd Catalyst System[a]

	Oxidation products/mmol		
[Cu]/[Pd]	CF_3COOCH_3	HCOOH	STY[b] × 10^3
0.0	—	—	—
1.0	0.15	0.31	2.6
2.5	0.24	0.40	3.6
5.0	0.32	0.54	4.8
50.0	0.25	0.11	2.0

[a] 5% Pd/C, 21.5 mg (Pd, 1.0×10^{-5} mol), $CuCl_2$ as Cu precursor; H_2O, 1 ml; CF_3COOH, 3 ml; CH_4, 300 psi; N_2, 100 psi; CO, 200 psi; O_2, 100 psi; 353 K; after 5 h.

[b] Same definition as described in Table 1.

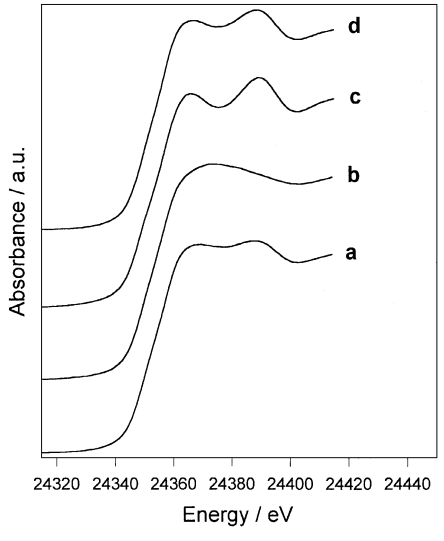

FIG. 8. Pd K-edge XANES of 5% Pd/C catalyst system with different mole ratios of $CuCl_2$ relative to Pd of 2.5 (a) and 5.0 (b) and 5% Pd/AC catalyst system reduced at 673 K before (c) and after the reaction (d) at a fixed amount of $CuCl_2$ ([Cu]/[Pd] = 5).

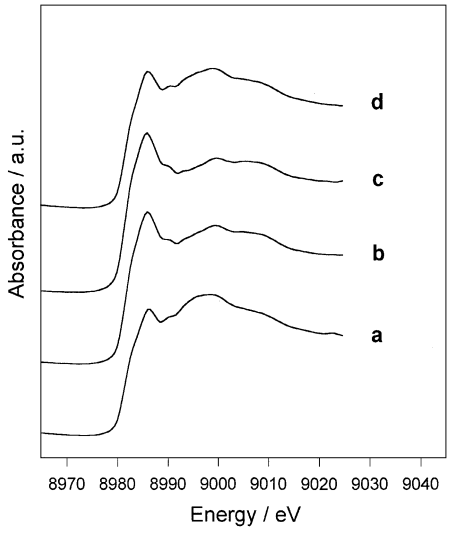

FIG. 9. Cu K-edge XANES of 5% Pd/C catalyst system with different mole ratios of $CuCl_2$ relative to Pd of 2.5 (a), 5.0 (b), and 50.0 (c) and 5% Pd/AC catalyst system reduced at 673 K after the reaction (d) at a fixed amount of $CuCl_2$ ([Cu]/[Pd] = 5).

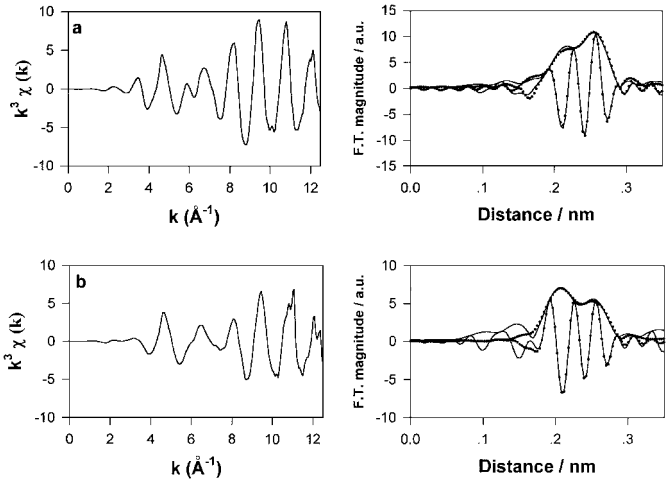

FIG. 10. k^3-weighted EXAFS functions and their Fourier transformation with the imaginary part about the Pd K-edge of 5% Pd/C catalyst system after the reaction with different mole ratios of $CuCl_2$ relative to Pd of 2.5 (a) and 5.0 (b). The EXAFS fitting results are plotted as dots. The solvent composition and reaction conditions were the same as those in Table 2.

of Pd/AC before and after the reaction were also compared in Fig. 8. Even in the presence of $CuCl_2$, the general features of the XANES spectrum for Pd/AC after the reaction looked like those of Pd metal.

In the case of Cu species, Fig. 9 compares Cu K-edge XANES of catalysts after the reaction with different amounts of $CuCl_2$. Cu K-edge XANES of catalysts after the reaction with poorly dispersed palladium was also displayed. In all cases, the peak below the edge at 8978 eV which served as a signature of a Cu(II) compound was not observed. Thus, it appears that Cu(II) compounds were reduced to Cu(I) compounds as also shown by XRD results. The edge positions of Cu samples were determined to be between 8981.0 eV and 8982.0 eV for all samples. This shift in edge position of copper also showed the reduction of the Cu(II) compound into a Cu(I) compound, which was consistent with the XRD pattern.

The effects of the amount of $CuCl_2$ on the structure of palladium were studied with EXAFS. Figure 10 shows the Pd K-edge EXAFS spectra of samples with different amounts of $CuCl_2$. Similarly to Fig. 6, both Pd–Cl and Pd–Pd interactions were evident in $\chi(k)$ and RSF, especially in imaginary parts of the Fourier transform. As the amount of $CuCl_2$ increased, the Pd–Pd peak decreased and the Pd–Cl peak became strengthened. The quantitative results of EXAFS fitting are shown in Table 4. As the amount of $CuCl_2$ per palladium increased from 2.5 to 5.0, the coordination number of Pd–Cl increased from 0.9 to 1.1 while that of Pd–Pd decreased from 4.0 to 1.1. Therefore, in agreement with the effect of NaCl, increasing amounts of $CuCl_2$ seem to cause the transition of palladium from the metallic state into the ionic state coordinated with Cl^-.

The effects of $CuCl_2$ on the structure of palladium for the catalyst with the low Pd dispersion were studied with EXAFS. Figure 11 shows the Pd K-edge EXAFS spectra of Pd/AC before (Fig. 11a) and after the reaction (Fig. 11b) in the presence of $CuCl_2$. After the reaction, Pd–Cl interaction appeared in RSF together with Pd–Pd coordination. The coordination number of Pd–Pd in Table 4 decreased from 8.8 for fresh catalyst to 6.0 for the catalyst after the reaction in the presence of $CuCl_2$. In the latter case, the coordination number of Pd–Cl was determined to be 1.5.

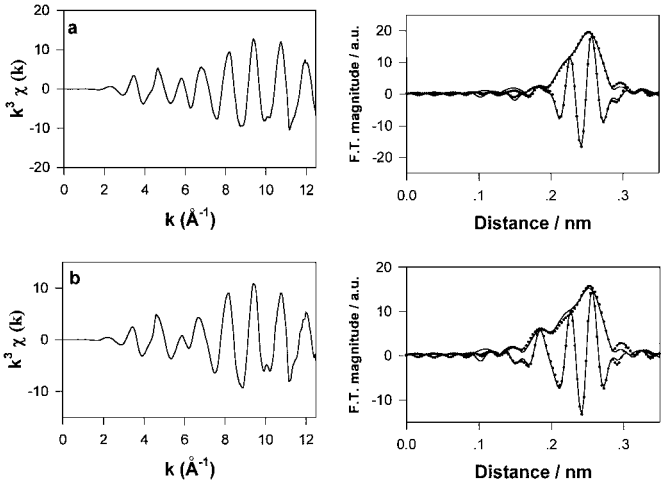

FIG. 11. k^3-weighted EXAFS functions and their Fourier transformation with the imaginary part about the Pd K-edge of 5% Pd/AC reduced at 673 K + $CuCl_2$ ([Cu]/[Pd] = 5.0) catalyst system before (a) and after the reaction (b). The EXAFS fitting results are plotted as dots. The solvent composition and reaction conditions were the same as those in Table 2.

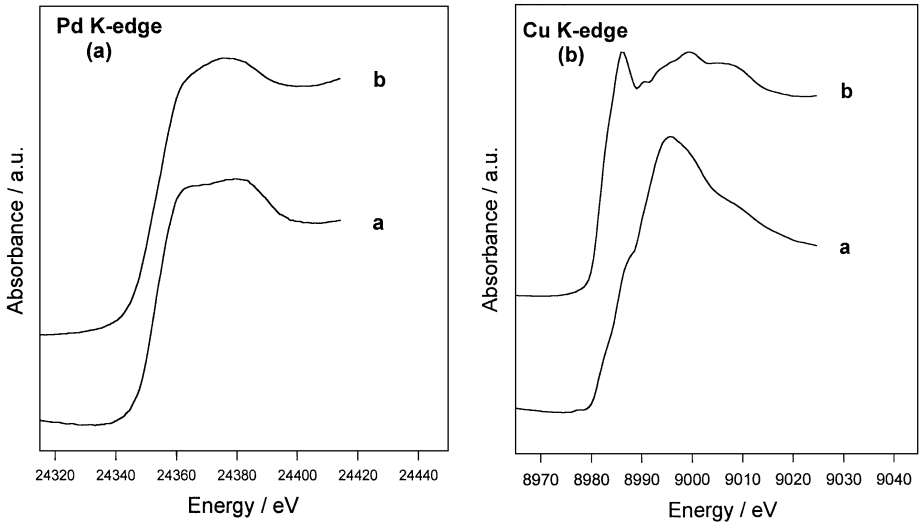

FIG. 12. Pd K-edge and Cu K-edge XANES of 5% Pd/C + $CuCl_2$ ([Cu]/[Pd] = 5.0) catalyst system in water (a) or TFA (b). The reaction conditions were the same as those in Table 2.

Solvent Composition

In this catalyst system, the solvent compositions have been reported to play an important role (6). We also observed that the maximum yield could be obtained in the mixture of water and TFA in the volume ratio of 1 : 3. When water was used as the sole solvent, carbon monoxide was oxidized a little but no methanol derivatives could be obtained. Furthermore, neither CO conversion nor formation of CF_3COOCH_3 was obtained when TFA was used as the sole solvent.

The effects of solvent composition on the structure of palladium were studied with XAFS techniques. In order to obtain information on the chemical state of Pd and Cu species in these catalysts after reactions with different solvent compositions, XANES spectra were obtained. Figure 12a compares Pd K-edge XANES of carbon-supported Pd catalysts after the reaction under different solvent compositions. In all cases, the general shapes of XANES of samples after the reaction appeared similar to that of $PdCl_2$.

In the case of Cu species, Fig. 12b compares Cu K-edge XANES of catalysts after the reaction with different solvent compositions. The peak below the edge at 8978 eV which serves as a signature of a Cu(II) compound was found after the reaction in water as the sole solvent. However, this peak could not be found after the reaction in TFA as the sole solvent. The edge positions of Cu samples were determined to be 8982.0 eV for the catalyst used in TFA. From these results, it was confirmed that Cu(II) compounds were reduced to Cu(I) compound in TFA but that Cu(II) compounds were dominant in water.

The effects of solvent compositions on the structure of palladium in the presence of $CuCl_2$ were studied with EXAFS. Figure 13 shows the Pd K-edge EXAFS spectra of samples in water-only and TFA-only solvent systems. The $\chi(k)$ and RSFs are both close to those of $PdCl_2$, irrespective of the solvent composition. However, the nonlinear fitting with only Pd–Cl scattering was unsuccessful for the catalyst used in TFA. Instead, the consideration of Pd–Pd coordination together with Pd–Cl interaction produced a good fitting as shown in Table 4. The small Pd–Pd coordination number of 0.3 indicates that the Pd–Cl interaction is dominant for the TFA-only solvent system as well as for the water-only solvent system.

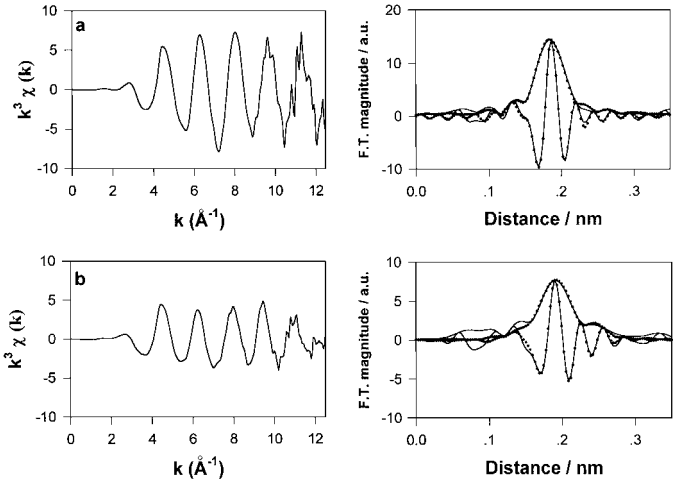

FIG. 13. k^3-weighted EXAFS functions and their Fourier transformation with the imaginary part about the Pd K-edge of 5% Pd/C + $CuCl_2$ ([Cu]/[Pd] = 5.0) catalyst system in water (a) or TFA (b). The EXAFS fitting results are plotted as dots. The reaction conditions were the same as those in Table 2.

DISCUSSION

Characterization of a novel catalyst of the type Pd/C–Cu was conducted with XRD and XAFS techniques. This catalyst was found to be active in functionalization of methane into a methanol derivative in the presence of CO and O_2 in agreement with the previous report (6). Its activity was also found to be strongly dependent on the nature of cocatalyst, halide ion, and the solvent composition (6). In this work, a systematic study or the reaction and catalyst characterization was conducted to correlate effects of the above variables on the catalytic activity with the structure and electronic state of palladium and copper.

Sen and co-workers (6) reported that Cu and Fe salts were effective promoters in the presence of Cl^- and selected Cu salts as better ones. They also screened halide ions for Cu salts and concluded that Cl^- was better than Br^- or I^-. From a separate screening test of promoters, we also observed that yields of a methanol derivative decreased in the order of $Cu(CH_3COO)_2 \gg Mn(CH_3COO)_2 > Co(CH_3COO)_2 > Ce(CH_3COO)_2 > PbO_2$ in the presence of NaCl. $FeCl_2$ appeared to be more effective than $Mn(CH_3COO)_2 + NaCl$ but much less effective than Cu(I) or Cu(II) salts. In the case of halide ion, the activity decreased in the order of $NaCl \gg NaF > NaBr > NaI$ in the presence of $Cu(CH_3COO)_2$ as a copper source. Therefore, the catalyst system of the type Pd–Cu–Cl was chosen as the most active one and was characterized intensively.

In the homogeneous catalyst system, a synergistic effect between Pd and Cu was confirmed by comparing run 3 with run 1 and run 2 in Table 1. The existence of Cl^- was also proved to be essential for the high activity and the nature of Cu compounds appeared to be important even in the presence of Cl^-.

Compared with the homogeneous noble metal catalyst system, the heterogeneous catalyst system has potential advantages including catalyst recovery. Thus, the heterogeneous Pd/C with different amounts of Cu(II) compounds and Cl^- and different solvent compositions were tested for the reaction and their structures were characterized. A linear relationship was obtained between yields of the methanol derivative and the amount of NaCl for the fixed amount of $Cu(CH_3COO)_2$ or the amount of $CuCl_2$ without added NaCl. This was not observed by Sen's group (6) because they used an excessive amount of NaCl or $CuCl_2$ per palladium (>35) in all cases. This increasing activity accompanied the change in the nature of the palladium and copper species. In the absence of NaCl, the coordination number of Pd–Pd increased during the reaction even in the presence of $Cu(CH_3COO)_2$. In the case of Cu salts, the reduction of the Cu(II) compound into Cu(I) did not occur even in the presence of excess CO over O_2. However, as the amount of NaCl increased, the coordination number of Pd–Pd decreased while that of Pd–Cl increased. Furthermore, Cu(II) was also reduced into Cu(I) species. These changes in catalysts are in line with increasing yields of the methanol derivative.

There have been a number of catalyst systems containing palladium and copper compounds that have synergistic effects in various reactions. Fujiwara and co-workers (32–35) reported that the Pd–Cu-catalyzed direct carboxylation of small alkanes such as methane, ethane, and propane proceeded electrophilically to give the corresponding carboxylic acids. In this reaction, the combination of $Pd(OAc)_2$ and $Cu(OAc)_2$ gave better yields than $Pd(OAc)_2$ alone. They characterized the $Pd(OAc)_2$–$Cu(OAc)_2$–$K_2S_2O_8$–CF_3COOH system (35) and found that $Pd(OCOCF_3)_2$ and $Cu(OCOCF_3)_2$ could be generated *in situ* and then a Pd–Cu(1 : 1) complex would be formed in which Pd was more positive than that in $Pd(OAc)_2$ alone. The Cu salt played an important role in strengthening the electrophilicity of $Pd(OAc)_2$. However, the presence of Cl^- was not required in this system and other reaction characteristics were quite different from those of the Pd/C–Cu system studied here.

The redox pair such as Pd–Cu has been reported in Wacker chemisty for the partial oxidation of ethylene and complete oxidation of CO (16–31). The overall chemistry of these oxidations in the catalytic system is believed to be similar to that of the well-known Wacker processes in the presence of a homogeneous $PdCl_2$–$CuCl_2$ catalyst:

$$C_2H_4\,(\text{or CO}) + PdCl_2 + H_2O \rightarrow CH_3CHO\,(\text{or } CO_2) + Pd(0) + 2HCl \quad [S1\text{-}1]$$

$$Pd(0) + 2CuCl_2 \rightarrow PdCl_2 + 2CuCl \quad [S1\text{-}2]$$

$$2CuCl + 2HCl + \tfrac{1}{2}O_2 \rightarrow 2CuCl_2 + H_2O. \quad [S1\text{-}3]$$

Initially, $PdCl_2$ is reduced to Pd(0) by ethylene or carbon monoxide, and then Pd(0) is reoxidized to $PdCl_2$ by $CuCl_2$. CuCl formed in reaction [2] is reoxidized to $CuCl_2$ by molecular O_2, which is also included in the feed gas stream. The presence of water is essential to sustain this catalytic cycle as shown above, and also was found experimentally to be so. The presence of Cl^- was also proved to be indispensable for the stabilization of molecular palladium and copper species to sustain this redox cycle (26). Differences in active catalysts between the synthesis of the methanol derivative and the partial oxidation lie in the chemical environments of palladium and the oxidation states of Cu salts. Both Pd–Pd and Pd–Cl interactions for the Pd side and a Cu(I) compound such as CuCl appeared to be dominant phases in active catalysts for the synthesis of the methanol derivative. However, only Pd(II) species coordinated with Cl^- and Cu(II) compounds such as $CuCl_2 \cdot 2H_2O$ or $Cu_2Cl(OH)_3$ were found in the partial oxidation.

Sen and co-workers (5, 6) observed the generation of H_2O_2 from CO and O_2 over 5% Pd/C in the acidified H_2O with HCl and also observed the similar oxidized products of hydrocarbons directly from H_2O_2 or from the CO–O_2–H_2O system. Therefore, they proposed that the overall transformation encompassed three catalytic steps as shown below (6):

$$CO + H_2O \rightarrow CO_2 + H_2 \qquad [S2\text{-}1]$$

$$H_2 + O_2 \rightarrow H_2O_2 \qquad [S2\text{-}2]$$

$$H_2O_2 + RCH_3 \rightarrow RCOOH + H_2O. \qquad [S2\text{-}3]$$

The first was water gas shift reaction involving the oxidation of carbon monoxide to carbon dioxide with the simultaneous formation of dihydrogen [S2-1]. The second catalytic step involved the combination of dihydrogen with dioxygen to yield hydrogen peroxide [S2-2]. The final step involved the metal-catalyzed oxidation of the alkane by hydrogen peroxide [S2-3]. From the characterization of 5% Pd/C by XRD and XAFS in this study, it was found that the agglomeration of the metallic palladium proceeded during the reaction without a Cu compound and Cl^-. An efficient functionalization of methane by Pd/C requires the presence of a copper compound and Cl^-. Both Pd(II) species and Pd(0) are present in the reaction system that gives high yields of CF_3COOCH_3.

From previous reports in the literature and our observations made here, the following reaction scheme composed of two parallel reactions for the Pd/C–Cu system could be proposed.

Reaction 1:

$$Pd(bulk) + 2CuCl_2 \rightarrow PdCl_2 + 2CuCl \qquad [S3\text{-}1]$$

$$2CuCl + \tfrac{1}{2}O_2 + 2HCl \rightarrow 2CuCl_2 + H_2O \qquad [S3\text{-}2]$$

$$PdCl_2 + CO + H_2O \rightarrow Pd(0) + CO_2 + 2HCl. \qquad [S3\text{-}3]$$

Reaction 2:

$$CO + H_2O \xrightarrow[[Pd(0)]]{} CO_2 + H_2 \qquad [S3\text{-}4]$$

$$H_2 + O_2 \xrightarrow[[Pd(0)]]{} H_2O_2 \qquad [S3\text{-}5]$$

$$H_2O_2 + CH_4 + CF_3COOH \xrightarrow[[Pd(II)]]{} CF_3COOCH_3 + 2H_2O. \qquad [S3\text{-}6]$$

Reaction 1 is CO oxidation by Wacker chemistry. Initially, bulk metallic palladium over carbon was oxidized into Pd(II) species coordinated with Cl^- by the Cu(II) species where the presence of Cl^- was proved to be essential [S3-1]. In the aqueous phase, the Wacker chemistry could proceed, which resulted in the complete oxidation of carbon monoxide into carbon dioxide as depicted in [S1-1, -2, and -3]. This side reaction consumes carbon monoxide which should be utilized for the *in situ* generation of H_2O_2 as shown in reaction 2. This complete CO oxidation can be accelerated by the presence of excessive amounts of Cl^- and $CuCl_2$ because these stabilize the Pd(II) species active for the reaction. Reaction 2 is the main route for the selective functionalization of methane. In the presence of TFA, the functionalization of CH_4 by Pd(II) species into CF_3COOCH_3 would be dominant as shown in [S3-6]. At this stage, the presence of H_2O_2 generated *in situ* over the metallic palladium from CO–O_2–H_2O appeared to be essential and its reaction scheme could be described as in [S3-4 and 5]. This is also supported by the previous observation that CF_3COOCH_3 could be obtained from CH_4 and H_2O_2 with $Pd(O_2CC_2H_5)_2$ in $(CF_3CO)_2O$ (47). There are two reaction schemes proposed for this stage [S3-6]. First, an electrophilic C–H activation over Pd(II) produces an organometallic intermediate CH_3–Pd(II) which is susceptible to a nucleophilic attack by CF_3COO^- followed by the reductive elimination of CF_3COOCH_3 (47). Second, Pd(II) activates peroxyacid generated *in situ* from H_2O_2 and CF_3COOH and leads to methane oxidation through a cyclic transition state composed of peroxyacid and methane (47). In both cases, the presence of H_2O_2 seems to be essential because these reactions did not proceed in the absence of CO or H_2O. In the case of an excessive amount of $Cu(CH_3COO)_2$ and NaCl or $CuCl_2$, CO was oxidized to a greater extent, but the yield of CF_3COOCH_3 was much less. This can be explained by the insufficient amount of metallic palladium that could not generate enough *in situ* H_2O_2 for the functionalization of CH_4 into CF_3COOCH_3 [S3-6]. Therefore, in this reaction system, the copresence of the metallic palladium and an ionized Pd(II) species stabilized by the presence of Cu salt and Cl^- appeared to be essential for the overall reaction to proceed effectively as shown above.

No methanol derivative was detected when either H_2O or CF_3COOH was utilized as the sole solvent as reported previously (6). In the absence of H_2O, the reaction scheme [S3-4 and S3-5] which is essential for the generation of *in situ* H_2O_2 cannot proceed. In the absence of CF_3COOH, only a small amount of CO was oxidized into CO_2, which might proceed as described in the reaction scheme from [S3-1] to [S3-3] similarly to the Wacker process for CO oxidation. The importance of CF_3COOH can be explained as follows. First, a methanol derivative (CF_3COOCH_3) produced from CH_4 and CF_3COOH can be stabilized by the electron-withdrawing CF_3COO group which will deactivate CF_3COOCH_3 not only toward electrophilic attack but also toward hydrogen atom abstraction. Second, CF_3COOH as a strong acid enhances the electrophilicity of the metal center because its conjugate base is a weak ligand. From EXAFS analysis, the coordination number of Pd–Pd for catalysts in either H_2O or CF_3COOH was found to be much smaller

than that for the catalyst in the mixture of CF_3COOH and H_2O. These structural data also indicate that the copresence of the metallic palladium and an ionized Pd(II) species which are essential for this reaction cannot be properly achieved in the absence of H_2O or CF_3COOH.

CONCLUSION

Carbon-supported Pd catalysts together with a copper compound were active for the oxidation of methane to a methanol derivative, CF_3COOCH_3, in the presence of CO and O_2. In this reaction system, the nature of cocatalyst, the presence of Cl^-, and the solvent composition changed the structure of palladium species and affected the yield of CF_3COOCH_3. In the presence of a copper compound and Cl^-, the metallic palladium can be partly oxidized into Pd(II) species, which resulted in higher yields of CF_3COOCH_3. For the active catalyst system, copper compound appeared to be present as CuCl. Pd(II) species coordinated with Cl^- appeared to be essential for the selective activation of methane and the metallic palladium for the *in situ* generation of H_2O_2 from CO, H_2O, and O_2.

ACKNOWLEDGMENTS

XAFS data were collected at the Photon Factory in the National Laboratory for High Energy Physics (KEK), Japan.

REFERENCES

1. Stahl, S. S., Labinger, J. A., and Bercaw, J. E., *Angew. Chem., Int. Ed.* **37**, 2180 (1998).
2. Periana, R. A., Taube, D. J., Gamble, S., Taube, H., Satoh, T., and Fujii, H., *Science* **280**, 560 (1998).
3. Periana, R. A., Taube, D. J., Evitt, E. R., Loffler, D. G., Wentrcek, P. R., Voss, G., and Masuda, T., *Science* **259**, 340 (1993).
4. Sen, A., *Platinum Metals Rev.* **35**(3), 126 (1991).
5. Lin, M., and Sen, A., *J. Am. Chem. Soc.* **114**, 7307 (1992).
6. Lin, M., Hogan, T., and Sen, A., *J. Am. Chem. Soc.* **119**, 6048 (1997).
7. Sen, A., *Acc. Chem. Res.* **31**, 550 (1998).
8. Fenton, D. M., and Steinwand, J., *J. Org. Chem.* **39**, 701 (1974).
9. Hallgren, J. E., Lucas, G. M., and Matthews, R. O., *J. Organomet. Chem.* **204**, 135 (1981).
10. Hallgren, J. E., and Lucas, G. M., *J. Organomet. Chem.* **212**, 135 (1981).
11. Heumann, A., Jens, K. J., and Reglier, M., *Prog. Inorg. Chem.* **42**, 542 (1994).
12. Vavasori, A., and Toniolo, L., *J. Mol. Catal. A: Chem.* **139**, 109 (1999).
13. Goyal, M., Nagahata, R., Sugiyama, J.-I., Asai, M., Ueda, M., and Takeuchi, K., *J. Mol. Catal. A: Chem.* **137**, 147 (1999).
14. Song, H. Y., Park, E. D., and Lee, J. S., *J. Mol. Catal. A: Chem.* **154**, 243 (2000).
15. Takagi, M., Miyagi, H., Yomeyama, T., and Ohgomori, Y., *J. Mol. Catal. A: Chem.* **129**, L1 (1998).
16. Smidt, J. R., Hafner, W., Jira, R., Sedlmeier, J., Sieber, R., Ruttinger, R., and Kojer, H., *Angew. Chem.* **71**, 176 (1959).
17. Miller, S. A., Ed. "Ethylene and Its Industrial Derivatives," p. 658. Ernest Benn, London, 1969.
18. Evnin, A. B., Rabo, J. A., and Kasai, P. H., *J. Catal.* **30**, 109 (1973).
19. Rao, V., and Datta, R., *J. Catal.* **114**, 377 (1988).
20. Lloyd, W. G., and Rowe, D. R., *Environ. Sci. Technol.* **5**(11), 1133 (1971).
21. Desai, M. N., Butt, J. B., and Dranoff, J. S., *J. Catal.* **79**, 95 (1983).
22. Choi, K. I., and Vannice, M. A., *J. Catal.* **127**, 489 (1991).
23. Kim, K. D., Nam, I.-S., Chung, J. S., Lee, J. S., Ryu, S. G., and Yang, Y. S., *Appl. Catal.: B* **5**, 103 (1994).
24. Koh, D. J., Song, J. H., Ham, S.-W., Nam, I.-S., Chang, R.-W., Park, E. D., Lee, J. S., and Kim, Y. G., *Korean J. Chem. Eng.* **14**(6), 486 (1997).
25. Lee, J. S., Park, E. D., and Song, B. J., *Catal. Today* **54**, 57 (1999).
26. Park, E. D., and Lee, J. S., *J. Catal.* **180**, 123 (1998).
27. Park, E. D., and Lee, J. S., *J. Catal.*, in press.
28. Lee, J. S., Choi, S. H., Kim, K. D., and Nomura, M., *Appl. Catal.: B* **7**, 199 (1996).
29. Choi, S. H., and Lee, J. S., *React. Kinet. Catal. Lett.* **57**, 227 (1996).
30. Yamamoto, Y., Matsuzaki, T., Ohdan, K., and Okamoto, Y., *J. Catal.* **161**, 577 (1996).
31. Park, E. D., and Lee, J. S., *Stud. Surf. Sci. Catal.*, in press.
32. Kurioka, M., Nakata, K., Jintoku, T., Taniguchi, Y., Takaki, K., and Fujiwara, Y., *Chem. Lett.* 244 (1995).
33. Nishiguchi, T., Nakata, K., Takaki, K., and Fujiwara, Y., *Chem. Lett.* 1141 (1992).
34. Nakata, K., Yamaoka, Y., Miyata, T., Taniguchi, Y., Takaki, K., and Fujiwara, Y., *J. Organomet. Chem.* **473**, 329 (1994).
35. Nakata, K., Miyata, T., Taniguchi, Y., Takaki, K., and Fujiwara, Y., *J. Organomet. Chem.* **489**, 71 (1995).
36. Hogan, T., Simpson, R., Lin, M., and Sen, A., *Catal. Lett.* **40**, 95 (1996).
37. Hogan, T., Simpson, R., Lin, M., and Sen, A., *Catal. Lett.* **49**, 59 (1997).
38. Pifer, A., Hogan, T., Snedeker, B., Simpson, R., Lin, M., Shen, C., and Sen, A., *J. Am. Chem. Soc.* **121**, 7485 (1999).
39. Sheldon, R. A., Ed. "Metalloporphyrins in Catalytic Oxidations." Dekker, New York, 1994.
40. Oyanagi, H., Matsishita, T., Ito, M., and Kuroda, H., KEK Report 83-30. 1984.
41. Nomura, M., KEK Report 85-7. 1985.
42. Nomura, M., and Koyama, A., KEK Report 89-16. 1989.
43. Rehr, J. J., Mustre, de Leon J., Zabinsky, S. I., and Albers, R. C., *J. Am. Chem. Soc.* **113**, 5135 (1991).
44. Wells, A. F., "Structural Inorganic Chemistry," 5th ed. Clarendon Press, Oxford, 1984.
45. Wells, A. F., *Z. Kristallogr.* **100**, 189 (1938).
46. Scherrer, P., *Gött. Nachr.* **2**, 98 (1918).
47. Kao, L.-C., Hutson, A. C., and Sen, A., *J. Am. Chem. Soc.* **113**, 700 (1991).